

Experimental Study on the Effect of Synchronization Accuracy for Near-Field RF Wireless Power Transfer in Multi-Antenna Systems

Gilles Callebaut*, Jarne Van Mulders*, Bert Cox*, Benjamin J. B. Deutschmann†, Geoffrey Ottoy*, Lieven De Strycker* and Liesbet Van der Perre*

**KU Leuven*, Belgium, gilles.callebaut@kuleuven.be, †*Graz University of Technology*, Austria

Abstract—Wireless power transfer (WPT) technologies hold promise for enhancing device autonomy, particularly for energy-limited IoT systems. This paper presents experimental results on coherent and non-coherent transmit diversity approaches for WPT, tested in the near field using the Techtile testbed. We demonstrate that a fully synchronized beamfocusing system achieves a 14 dB gain over non-coherent transmission, consistent with the theoretical 14.9 dB gain for a 31-element array. Additionally, phase alignment errors below 20° result in less than 1 dB of gain loss, while errors exceeding 40° lead to losses over 3 dB. These findings suggest that phase coherency requirements for WPT can be relaxed, and that scaling the number of antennas is a promising strategy for improving power transfer efficiency. **Index Terms**—beamfocusing, distributed MIMO, energy-neutral devices, near-field WPT, wireless power transfer

I. INTRODUCTION

Wireless power transfer (WPT) technologies hold a great potential to increase autonomy of devices in a very convenient way. They have attracted ample attention in view of the growing number of deployed energy-limited Internet of Things (IoT) devices. Ultimately, they could provide a theoretically infinite lifetime and enable energy-neutral operation of the IoT devices, i.e., the delivered energy fully covers the consumption needs of the devices. Many studies have addressed the main challenges related to getting sufficient energy across and increasing the efficiency of the wireless power transfer (WPT), covering aspects such as, signals and systems or hardware solutions [2–5]. Large and distributed antenna systems open interesting new opportunities to focus the power in beams and spots [6, 7]. In particular, coherent approaches have been shown to theoretically provide spectacular improvements in transfer efficiency. However, these systems require a couple of tough problems to be resolved, including the acquisition of channel state information (CSI) [8] and the synchronization of many distributed transmitters [9], among others. To combat these challenges, non-coherent approaches are being proposed for multi-antenna systems. An example is employing phase sweeping transmit diversity [10–12]. In this method, the antennas do not require CSI and only transmit phase-shifted signals at a single carrier. We have experimentally

studied this technique and others in our testbed Techtile [13] in the RF near-field* and report on the promising results in this paper. Furthermore, We have performed experiments to validate the beamfocusing capabilities of distributed multiple-input multiple-output (MIMO) transmission for WPT with different degrees of phase accuracies. The results confirm the theoretical beamfocusing gains for both non-coherent and coherent WPT and confirm the hypothetical power spot size of $\lambda/2$. This raises the confidence level that, scaling up the number of antennas, is an effective strategy. Moreover, the experiments show that phase alignment errors of up to 20°, still allow to achieve beamfocusing gains, with only a loss of 1 dB with respect to the fully coherent case with a 31-element array, yet the losses rapidly increase beyond 40° errors.

This paper is further organized as follows. In the next section, we explain the experimental environment and conditions and in particular the approach to achieve synchronized transmission. The investigated wireless power transfer (WPT) strategies and experiments are introduced in Section III and Section IV respectively. The measurements results and their evaluation are presented in Section V. Finally, Section VI summarizes the main conclusions of this study and provides an outlook for future work.

II. TECHTILE EXPERIMENTAL ENVIRONMENT AND SYNCHRONIZATION APPROACH

A. Techtile Testbed

The Techtile measurement infrastructure [13] (Fig. 1) serves as a versatile, multi-functional testbed for experimental research on innovative communication, positioning, sensing, and federated learning technologies exploiting spatially distributed resources. Modularity is achieved by constructing the ceiling, floor, and walls out of 140 detachable tiles. Each tile is equipped with a custom power-over-Ethernet (PoE) board with power supply up to 90 W, a universal software radio peripheral (USRP) B210 with two antennas and a Raspberry Pi 4 for edge processing. The backbone of Techtile consists of a central server, enabling communication, sub-microsecond time synchronization and power to all tiles over a single Ethernet

The work is supported by the REINDEER project under grant agreement No. 101013425 and by the e-construct project under the *Vlaams Agentschap Innoveren en Ondernemen (VLAIO) grant agreement HBC.2021.0911.

Manuscript accepted on 12 December 2024 for 2025 19th European Conference on Antennas and Propagation (EuCAP) [1].

*Note, in this work, the term *near-field* refers specifically to the electric near-field region of the antenna array. While *near-field* in the context of WPT often implies electromagnetic coupling-based charging, this interpretation does not apply to our study.

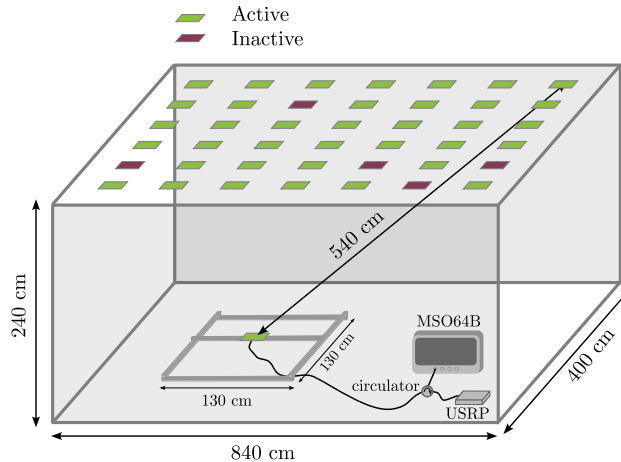


Fig. 1: Picture and illustration of the experimental set-up Techtile [13], with transmitters on the ceiling and a movable antenna connected to the measurement equipment. The movable antenna allows to spatially sample the received power over a grid of 130 by 130 cm.

TABLE I: Overview of WPT strategies, their used acronyms in figures, the applied downlink transmit phase and the synchronisation requirement needed to provide radio frequency (RF) WPT.

Acr.	RF WPT Strategy	Applied TX phase	Short description	Sync. Requirements		
				Time	Freq.	Phase
BF	beamfocusing (near-field) or beamforming (far-field)	$-\hat{\varphi}$	In the beamfocusing strategy, reciprocity-based downlink WPT is used, where the phase $\hat{\varphi}$ at all antennas is estimated using an uplink pilot.	✓	✓	✓
SISO	single antenna	N.A.	Only one antenna is used during transmission.	✗	✗	✗
RPS	Random-phase sweeping	$\varphi_{AS} \sim \mathcal{U}(0, 2\pi)$	All transmitters change their phase every 10 ms at the same carrier frequency.	✓	✓	✗
G-BF	BF with Gaussian noise	$-\hat{\varphi} + \varphi_{G-BF}$	After uplink training, each antenna adds a phase $\varphi_{G-BF} \sim \mathcal{N}(0, \sigma_{\varphi}^2)$ drawn from a normal distribution. This is used to study the effect on the accuracy of the phase synchronization.	✓	✓	±

connection. An in-depth review on the multi-functionality of Techtile can be found in [13]. Since the publication of [13], the testbed has been extended with new hardware facilitating:

- Sub-centimeter 3D positioning and tracking accuracy thanks to the Qualisys motion capture system.
- Accurate time and frequency synchronization through local oscillator (LO) distribution.
- Automatic 2D spatial sampling due to the OpenBuilds ACRO CNC system.

B. Synchronization Capabilities of Techtile

This work examines various levels of synchronization, made possible by Techtile's capabilities in achieving a phase-coherent system. The methods used for time, frequency, and phase synchronization are outlined below.

1) *Time Synchronisation*: Time synchronization is achieved by distributing a pulse per second (1PPS) signal to all USRPs using Octoclocks. Before starting a measurement, an absolute time is agreed upon by all USRPs. To facilitate this, the USRPs participating in the experiment connect to the same ZeroMQ (ZMQ) server. After establishing the connection, the server sends a start command, which is received by all USRPs within a few milliseconds. Upon receiving the command, each USRP waits for a 1PPS trigger, at which point the time is set to zero,

thereby establishing a common absolute time frame. From this point forward, all USRPs operate on the same time reference, and subsequent commands are executed at specific times to maintain time synchronization.

2) *Frequency Synchronisation*: Frequency synchronisation is achieved through the distribution of a 10 MHz signal using Octoclocks to all USRPs. This reference clock is used to synthesize the required clocks on the field-programmable gate array (FPGA) and transceiver.

3) *Phase Synchronisation*: The USRP B210 devices have two separate LOs to work in frequency-division duplexing (FDD) mode, i.e., transmitting and receiving simultaneous on two distinct frequencies. In the case of the USRP B210, this results in a TX and RX LO that are not phase-locked, i.e., the phase relation between the two LO is unknown and nondeterministic.[†] However, this phase relation is required to perform coherent downlink beamforming. It relies on the fact that the transmit and receive frontends are reciprocal, i.e., the phase relation between them is known. In this setup, the phase differences (due to path lengths and electrical components)

[†]To be complete, if the software-defined radios (SDRs) are configured in *integer phase-locked loop (PLL) mode*, the phase relation between the SDRs are deterministic due to the dividers present in the RF chains.

between the TX and RX frontends and LOs are measured. More details regarding the reciprocity calibration can be found in [\[9\]](#).

III. MULTI-ANTENNA RF WPT STRATEGIES

In this work, we are studying the effect of the level of synchronization accuracy required to perform RF WPT in distributed systems. Four different strategies are considered and summarized in Table I. Each of those strategies requires a different synchronization level.

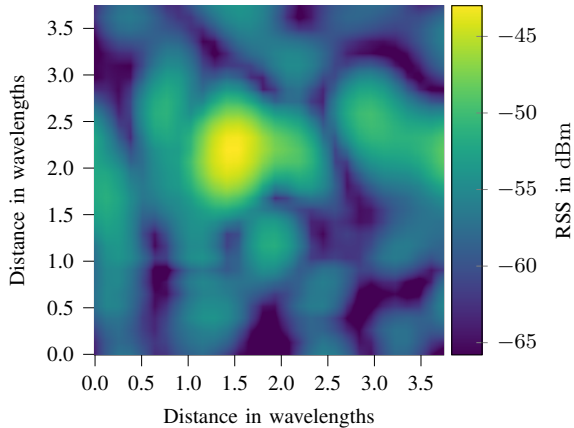


Fig. 2: Heatmap of the received signal strength (RSS) resulting from coherent beamforming (BF), measured with the movable receive antenna over the full grid. The power spot is approximately $\lambda/2$ in diameter (when considering a -3 dB power threshold).

A. Single-input single-output (SISO)

The single-input single-output (SISO) strategy is included in this work as a benchmark to compare the obtained gains of the other strategies. In the SISO case, only one antenna is used to perform WPT. Hence, no form of synchronization is required.

B. Random-Phase Sweeping (RPS)

When the system is not phase-coherent, but provides time and frequency synchronization, random-phase sweeping can be used to illuminate dead spots.[‡] By randomly changing the phase of all antennas at regular intervals, fluctuations in the received power can be induced, yielding different levels of constructive interference at different time and spatial instances. This is especially interesting when the average received power is below the required threshold for a device to get charged. A peak in power could “jump start” the device. Multi-carrier systems are examples where the different carriers induce large fluctuations, yielding high peak-to-average power ratio (PAPR) signals. However, in recent studies, single-carrier transmissions with adaptive phase-changes have shown to be more promising than multi-carrier systems for energy-neutral devices (ENDs) [12].

[‡]github.com/techtile-by-dramco/NI-B210-Sync

[§]Furthermore, this strategy can also be employed if the device is unable to send and uplink pilot and its location is unknown.

When transmitting with the same power, the statistical expectation of the power gain with respect to SISO is the sum of the received powers of all individual antennas [14]. This is sometimes also called the non-coherent gain. In literature, the gain is often expressed as $10 \log_{10}(M)$, with M the number of antennas. This is the case when the large-scale fading from all antennas to the device are the same. However, in near-field, the distributed antennas experiences different large-scale fading.

C. Near-Field Beamfocusing (BF)

In a fully coherent system, the phase relations between all antennas are known. Hence, these systems need to be time, frequency, and phase synchronized. In the case when the devices are located in the near-field of the system, the term beamfocusing is used, while when operating in the far-field, beamsteering is used. In the latter case, under line-of-sight (LoS) conditions and for a single user, the antenna array physically forms a beam directed toward the desired user. However, in the near-field, the received signals have a spherical wavefront, illuminating a specific spot rather than forming a beam, which is why the term beamfocusing is commonly used in the literature. Analogously, beamsteering acts like a flashlight, while beamfocusing resembles a spotlight. The term beamforming will be used as a general term to depict both beamsteering or beamfocusing, depending on the near- or far-field condition.

In our setup, beamfocusing is performed by estimating the phase $\hat{\varphi}$ of the received signal at all antennas, through a single-tone uplink signal transmitted by the device. This device will be called END in the remainder of this manuscript. This indicates that it is the target device, where we want to transfer energy to. When performing downlink WPT, the opposites of the estimated phases are applied when transmitting a single-carrier tone at all antennas, yielding constructive interference at the target location/END. The corresponding “spotlight” will be called the power spot or focal region. This considered region is the area where the received power level is not lower than 3 dB with respect to the target location. Such a power spot is visible in Fig. 2.

When transmitting with the same power, the expected gain with respect to a SISO[¶] system is $20 \log(M)$ and $10 \log(M)$ compared to the RPS approach.

D. Beamfocusing with phase errors (G-BF)

While G-BF is technically not a WPT technique, the performance degradation with respect to the achievable phase-coherency case is studied by artificially applying a phase error to the estimated uplink phase. It allows evaluating the loss in gain with respect to the fully phase-coherent system. The applied transmit-phase during downlink WPT is determined as,

$$-\hat{\varphi} + \varphi_{\text{G-BF}},$$

[¶]In literature $10 \log(M)$ is used, as they assume that with M antennas the transmit power is also M times lower, which is not considered in this work.

where $\hat{\varphi}$ is the estimate of the uplink pilot phase and $\varphi_{\text{G-BF}} \sim \mathcal{N}(0, \sigma_\varphi^2)$ is a random phase drawn from a normal distribution with standard deviation σ_φ .

When the standard deviation is high, this yields on average (in space and time) the same results as the **RPS**. However, **G-BF** would result in a constant received power, as the phase is constant during WPT, which could be potentially a dead spot. While in **RPS**, due to the constantly changing phases, the same location would experience different power levels during WPT.

IV. EXPERIMENTS

The aforementioned Techtile infrastructure is used to compare the proposed wireless power strategies in a real world environment. To confine the measurement size, the received power is measured in a 2D plane of 130 cm × 130 cm, as sketched in Fig. 1. At the infrastructure side, 1 or 31 of the distributed patch antennas in the ceiling transmit a 920 MHz continuous sine wave with a transmit power of 3 dBm. Depending on the strategy, the transmitters are time and/or phase synchronized. For reciprocity-based downlink transmission, an uplink pilot is used to determine the received phase at each antenna, as detailed in Section III-C.

The antenna at the END side is moved by the ACRO CNC machine in the delimited plane. The same patch antenna is used at the device and infrastructure side and are orientated towards each other. This enables repetitive received power measurements. As can be seen in Fig. 1, the END antenna is connected via a circulator to the oscilloscope and END USRP. The circulator ensures that the transmitted signal from the USRP is transmitted via the antenna, while the receive signals are relayed to the Tectronix MSO64B oscilloscope to measure the received power. The exact position and orientation of the receiver is obtained through the Qualisys system. The processing scripts and data can be found on [GitHub](#)¹.

V. EVALUATION

The strategies are evaluated based on the received signals strength in the power spot and its size. Additionally, the effect of the synchronization level on the average power inside and outside the focal region is investigated.

A. Power spot size

As can be observed in Fig. 2, **the created power spot (BF) has a diameter of approximately $\lambda/2$ in diameter.**** This means, that outside of this area, the received power is lower than 3 dB with respect to the target location. This is in line with the theoretical expectation of the power spot size [15].

B. Effect of synchronization accuracy on the average received power

The impact on the system synchronization capability/accuracy for the received power in the focal region can be seen in Fig. 3. **In case of a fully synchronized system (BF), the average**

¹github.com/techtile-by-dramco/experiments/tree/main/02_reciprocity_based_WPT

**The measured power spot area is 0.03 m².

received power is -45 dBm. This is 14 dB higher than the RPS case, which is in line with the expected gain of 14.9 dB (corresponding to $10 \log_{10}(M)$), as outlined in Section III-C. In turn, the **RPS** strategy has a gain of 7 dB with respect to the **SISO** case. Note that here the **SISO** antenna is the one closest to the target location and thus has the largest path gain.

With an increased phase error (**G-BF**), the received power is decreasing, moving closer to the **RPS** case, as can be seen when comparing the P50 of the **G-BF** to the **RPS** plot. The P50 of the **G-BF** allows to investigate the loss in gain when having a certain degree of phase error. As can be observed, **for low standard deviations of the phase error (below 20°), the gain loss is below 1 dB.** As of 40°, we have a gain loss higher than 3 dB. **This observation is promising for WPT, indicating that the phase-coherency requirements can be relaxed.** These observations are again in line with theoretical expectations [16]. Notably, the same conclusions cannot be made for communication, which would require tighter synchronization.

C. Effect of synchronization accuracy on the distribution of received power

In most cases, we want to have as much power as possible in the intended location and as low as possible outside. The distribution, and more specifically the cumulative distribution function (CDF), of the received powers for the different synchronization accuracies is shown in Fig. 4. The figure provides the received powers sampled in the full grid, as indicated in Fig. 1. This for both inside the focal region, i.e., an area of $\lambda/2$ by $\lambda/2$ around the target location, and outside the focal region.

Observations:

- 1) In the **SISO** case, the received power is higher inside the focal region than outside. This is because the SISO antenna is positioned directly above the focal region. Hence, more power is expected right below the SISO transmit patch antenna.
- 2) The **BF** strategy results in the highest maximum and lowest minimum received power. “Dark spots” are created outside the focal region, having powers as low as -100 dBm (which is close to the measured noise floor). On the other hand, inside the focal region, the received powers are maximized, as also visible in Fig. 2.
- 3) For **G-BF**, the small width of the CDF indicates that the received powers within the focal region are very similar in the power spot area. This is a result of the phase noise added to the transmitted phases, which broadens the power spot, effectively smudging out the power spot. This effect is also observed and leveraged on in [8].
- 4) **RPS** exhibits a similar power distribution both inside and outside the BF region, which is expected since the **RPS** approach induces rapid power fluctuations that, when averaged over time, ideally occur uniformly across all positions. In some cases, higher power is observed in the BF region when using **RPS** compared to **G-BF** with a phase error standard deviation of $\pi/2$. This suggests

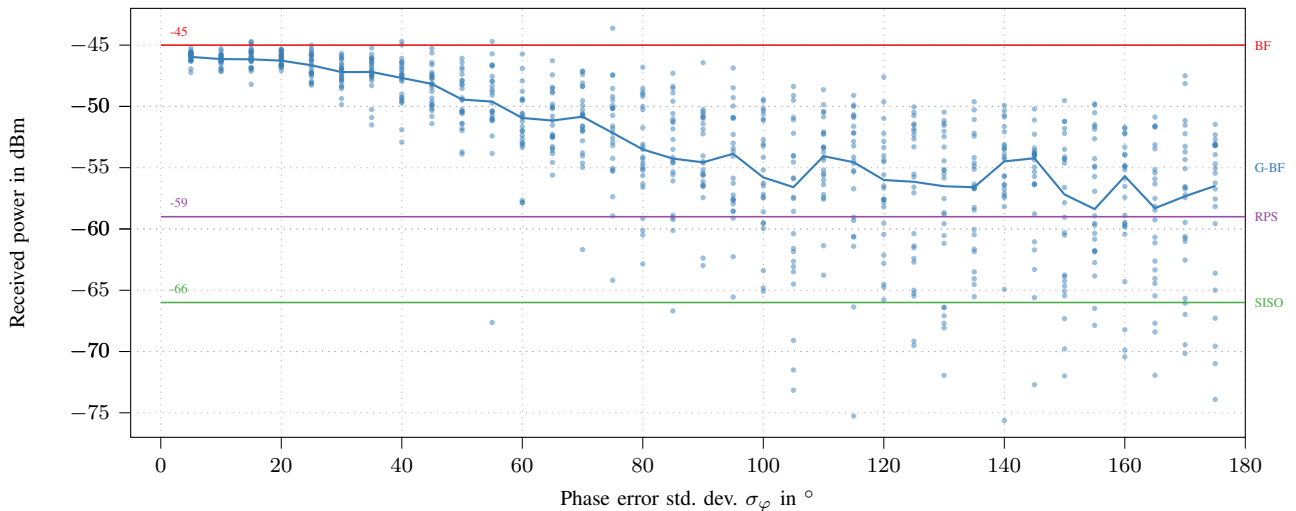


Fig. 3: The RSS in the case of SISO, RPS, and BF is plotted for a single location). The phase synchronization accuracy (G-BF) is evaluated by adjusting the transmit phase as described in Section III-D, each point represents one realization of the random phases and the line depicts the median (P50). Each realization yields a potential different receive power. The standard deviation of the phase error in degrees is on the x-axis.

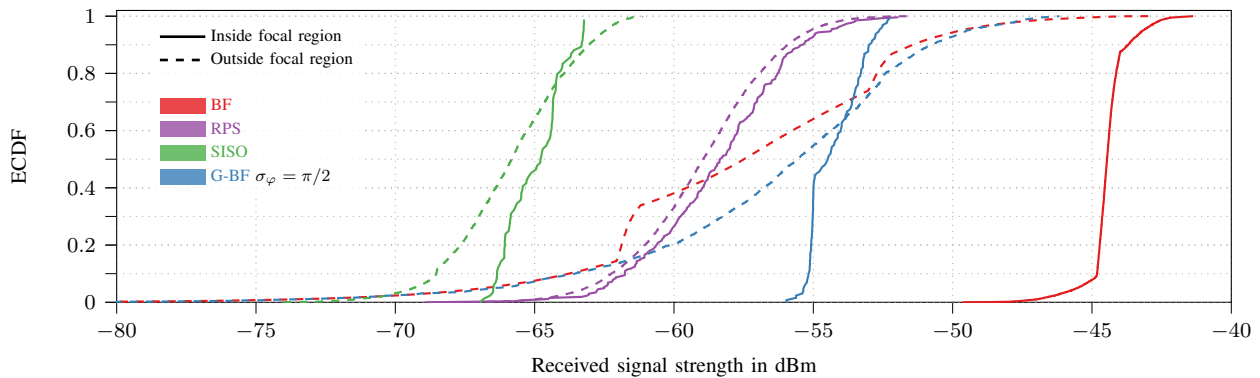


Fig. 4: Empirical cumulative distribution function (eCDF) of the measured received power using the movable END antenna across the full grid for all studied strategies WPT. The received powers outside and inside the focal region are plotted separately. The x-axis is limited to -80 dBm to enhance readability, although power samples drop as low as -100 dBm for the BF strategy outside the focal region. The plot allows to examine i) the gain in the power spot region, ii) the power spread, and iii) the potential reduction in received power outside the target location in case of the BF strategy.

that **RPS could be preferable in scenarios with low synchronization, where peak power is more desirable than average power**, as is sometimes the case for ENDS [12].

VI. CONCLUSIONS AND FUTURE OUTLOOK

This paper has reported on an experimental study of distributed beamforming for RF-based wireless power transfer (WPT). In particular, a coherent approach is pursued. The results validate and demonstrate the great gains that can be achieved in efficiency as predicted in theory. The beam focusing capability is clearly present in the visualization of the measured receive power levels. An important condition to realize the power transfer efficiency gain is accurate synchronization of the transmitters, which poses a harsh challenge in practical deployments. Fortunately, the results indicate the promise of only small performance degradations even when having a standard deviation of the phase error as high as 40° , with only a 3dB loss. This would indicate that the update rate

of the calibration and channel state information (CSI) estimation procedure could be lowered for radio frequency (RF) WPT. The current status is promising to enhance coverage and service levels for interaction with energy-neutral devices relying on RF-based WPT. It calls for further R&D efforts to progress low-complexity elegant solutions for achieving accurately synchronized transmitters. Furthermore, the scaling up towards more antennas and more devices to be serviced, poses additional challenges in terms of coordination, protocols and scheduling to be resolved.

ACKNOWLEDGEMENTS

The authors would like to thank Thomas Wilding from TU Graz for his valuable discussions on the subject, and Guus Leenders and François Rottenberg from KU Leuven for the help on getting Tectile synchronized.

REFERENCES

- [1] G. Callebaut *et al.*, “Experimental study on the effect of synchronization accuracy for Near-Field RF wireless power transfer in Multi-Antenna systems,” in *2025 19th European Conference on Antennas and Propagation (EuCAP) (EuCAP 2025)*, Stockholm, Sweden, Mar. 2025, p. 4.98.
- [2] J. Huang *et al.*, “Wireless Power Transfer and Energy Harvesting: Current Status and Future Prospects,” *IEEE Wireless Communications*, vol. 26, no. 4, pp. 163–169, 2019.
- [3] M. Wagih *et al.*, “Rectennas for Radio-Frequency Energy Harvesting and Wireless Power Transfer: A Review of Antenna Design [Antenna Applications Corner],” *IEEE Antennas and Propagation Magazine*, vol. 62, no. 5, pp. 95–107, 2020.
- [4] J. Van Mulders *et al.*, “Wireless Power Transfer: Systems, Circuits, Standards, and Use Cases,” *Sensors*, vol. 22, no. 15, 2022.
- [5] Y. Zeng *et al.*, “Communications and Signals Design for Wireless Power Transmission,” *IEEE Transactions on Communications*, vol. 65, no. 5, pp. 2264–2290, 2017.
- [6] H. Zhang *et al.*, “Near-Field Wireless Power Transfer for 6G Internet of Everything Mobile Networks: Opportunities and Challenges,” *IEEE Communications Magazine*, vol. 60, no. 3, pp. 12–18, 2022.
- [7] S. D. Van *et al.*, “Wireless Powered Wearables Using Distributed Massive MIMO,” *IEEE Transactions on Communications*, vol. 68, no. 4, pp. 2156–2172, 2020.
- [8] B. J. B. Deutschmann *et al.*, “XL-MIMO Channel Modeling and Prediction for Wireless Power Transfer,” in *2023 IEEE International Conference on Communications Workshops (ICC Workshops)*, 2023, pp. 1355–1361.
- [9] E. G. Larsson, “Massive Synchrony in Distributed Antenna Systems,” *IEEE Transactions on Signal Processing*, vol. 72, pp. 855–866, 2024.
- [10] A. Hiroike *et al.*, “Combined effects of phase sweeping transmitter diversity and channel coding,” *IEEE Transactions on Vehicular Technology*, vol. 41, no. 2, pp. 170–176, 1992.
- [11] B. Clerckx *et al.*, “On the Beneficial Roles of Fading and Transmit Diversity in Wireless Power Transfer With Nonlinear Energy Harvesting,” *IEEE Transactions on Wireless Communications*, vol. 17, no. 11, pp. 7731–7743, 2018.
- [12] J. Van Mulders *et al.*, “Single versus Multi-Tone Wireless Power Transfer with Physically Large Arrays,” in *2024 1st International Workshop on Energy Neutral and Sustainable IoT Devices and Infrastructure (EN-IoT 2024)*, Paris, France, Oct. 2024, p. 5.98.
- [13] G. Callebaut *et al.*, “Techtile – Open 6G R&D Testbed for Communication, Positioning, Sensing, WPT and Federated Learning,” in *2022 Joint European Conference on Networks and Communications & 6G Summit (EuCNC/6G Summit)*, 2022, pp. 417–422.
- [14] J. Van Mulders *et al.*, “Keeping Energy-Neutral Devices Operational: a Coherent Massive Beamforming Approach,” in *2024 IEEE 25th International Workshop on Signal Processing Advances in Wireless Communications (SPAWC) (IEEE SPAWC 2024)*, Lucca, Italy, Sep. 2024, p. 4.97.
- [15] L. Van der Perre *et al.*, “RadioWeaves for efficient connectivity: analysis and impact of constraints in actual deployments,” in *2019 53rd Asilomar Conference on Signals, Systems, and Computers*, 2019, pp. 15–22.
- [16] REINDEER project, “Hardware requirements to support energy transfer to energy-neutral nodes,” Deliverable ICT-52-2020 / D2.3, unpublished (2023).